

In the format provided by the authors and unedited.

# Distinct mechanisms coordinate transcription and translation under carbon and nitrogen starvation in *Escherichia coli*

Sukanya Iyer<sup>1</sup>, Dai Le<sup>1</sup>, Bo Ryoung Park<sup>1</sup> and Minsu Kim<sup>1,2,3\*</sup> 

---

<sup>1</sup>Department of Physics, Emory University, Atlanta, GA, USA. <sup>2</sup>Graduate Division of Biological and Biomedical Sciences, Emory University, Atlanta, GA, USA. <sup>3</sup>Emory Antibiotic Resistance Center, Emory University, Atlanta, GA, USA. \*e-mail: [minsukim@emory.edu](mailto:minsukim@emory.edu)

## **Supplementary information**

**Title:** Distinct mechanisms coordinate transcription and translation under carbon and nitrogen starvation  
in *E. coli*.

**Author:** Sukanya Iyer, Dai Le, Bo Ryoung Park, and Minsu Kim

## Supplementary Methods

### Strain construction

In NMK80, the expression of a *lacZ* reporter gene was controlled by a synthetic promoter  $P_{LTet-O1}$  ( $P_{LTet-O1-lacZ}$ )<sup>1</sup>. Construction of this strain was described elsewhere<sup>2</sup>. We received the pALS13 plasmid<sup>3</sup> and strain CF15004 which contains the *spoT E319Q* allele (associated with Zib 256::Tn10)<sup>4</sup> from Dr. Michael Cashel. We transformed NMK80 with the pALS13 plasmid, creating NMK156. Transducing the *spoT E319Q* allele to NMK80 using P1 transduction<sup>5</sup>, we created NMK215. We amplified the  $P_{tac-relA}$ ' cassette in the pALS13 plasmid using the primer named *tac\_rela\_fwd* and *rela\_kan\_rev*. See Supplementary Table 3 for sequences of all the primers used. Kanamycin resistance gene was amplified from the pKD13 plasmid<sup>6</sup>, using the primers *kan\_fwd* and *kan\_rela\_rev*. The PCR products were then fused using fusion PCR, using the primers *ins\_tac\_rela\_fwd* and *ins\_rela\_rev*. The PCR cassette was electroporated into the NMK 215 cells containing pKD46. Kanamycin-resistant colonies were selected and the presence of  $P_{tac-relA}$ ' was verified by PCR and Sanger sequencing. The resulting strain was named NMK217.

### Supplementary Note 1

Cells lacking peptidase activities lose viability rapidly upon starvation<sup>7</sup>. The measurement of WT cells showed high rates of protein degradation during the early hours of starvation (a few hours)<sup>7</sup>. Interestingly, WT cells also exhibit high rates of new protein synthesis during the early hours of starvation<sup>8</sup>. The inhibition of protein synthesis in the early hours of starvation has detrimental effects on cell survival, whereas the inhibition at later times has only limited effects<sup>9</sup>. The newly synthesized proteins are involved in alterations of the composition/structure of cell membrane and peptidoglycan or energy generation for long-term survival without cell growth<sup>10-15</sup>. Also, starvation was shown to lead to oxidative damage to cells<sup>16-19</sup>, and proteins protecting cells from oxidative stress are synthesized during starvation<sup>20,21</sup>.

### Supplementary Note 2

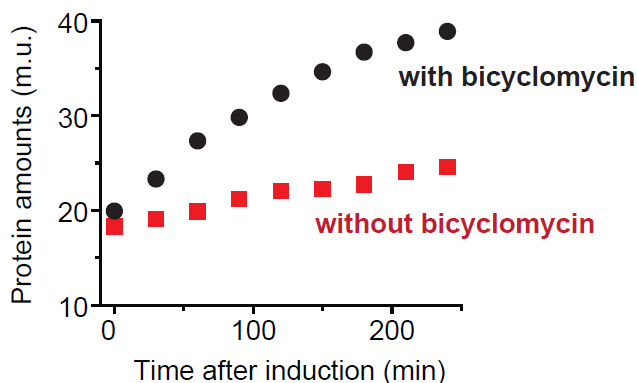
What determines transcription elongation speed in starved cells treated with chloramphenicol is an interesting question. The primary effect of chloramphenicol is inhibition of translation. Because transcription relies on translation during C-starvation, translation inhibition by chloramphenicol leads to a slowdown of transcription elongation (green bars in Fig. 2c). However, transcription does not rely on translation during N-starvation. Thus, translation inhibition by chloramphenicol does not lead to a slowdown of transcription elongation (blue bars in Fig. 2c). Interestingly, early in N-starvation (10 mins),

transcription elongation is a bit higher with than without chloramphenicol treatment; compare the solid and open blue bars at 10 mins in Fig. 2c. This marginal difference could be explained by a known effect of chloramphenicol on (p)ppGpp levels together with our findings regarding the effects of (p)ppGpp on transcription elongation. Without chloramphenicol treatment, (p)ppGpp concentrations reach their maximum values within 10 mins after starvation<sup>22-24</sup>. Previous studies have shown that chloramphenicol treatment results in a decrease in (p)ppGpp levels<sup>25-27</sup>. Our experiments using the (p)ppGpp-overexpressing strain (NMK156) and (p)ppGpp-defective strain (NMK217) showed that a decrease in (p)ppGpp levels causes an increase in transcription elongation speed (Fig. 3a and Supplementary Fig. 12). Therefore, early in N-starvation, transcription elongation speed is expected to be higher with chloramphenicol treatment, because the treatment leads to a decrease in (p)ppGpp levels and this decrease causes an increase in transcription elongation speed. Note that (p)ppGpp concentrations decrease to low levels later in starvation regardless of chloramphenicol treatment<sup>22-24</sup>, which is why we do not see a difference in the speed at 45 mins in Fig. 2c.

### **Supplementary Note 3**

Our extensive characterization has shown that *lacZ* mRNA tails are hybridized as well as the head (see Fig. 2-3 in our previous article<sup>2</sup>, and also compare Fig. 1b and Supplementary Fig. 5 in this work); therefore, the fact that we did not observe hybridization signals from tails strongly suggests the absence of tails. It is possible that the tails were produced but degraded. When we characterized the degradation of mRNA molecules, we observed that mRNA heads disappeared first and after a time delay, mRNA tails disappeared (Fig. 3b in our previous article<sup>2</sup>); such a time delay was previously reported by others as well<sup>28</sup>. Therefore, degradation would lead to the disappearance of both heads and tails or disappearance of just heads. To further support premature termination, we treated cells with bicyclomycin, a selective inhibitor of Rho (Rho is an important protein involved in premature termination). We found that the treatment led to an increase in LacZ expression (the results were shown in Supplementary Fig. 1). Lastly, in the field, the presence of mRNA heads but absence of tails are taken as a sign of premature termination (we briefly summarized previous studies of premature termination in Supplementary Fig. 1 caption. Please see the reference therein). Collectively, these pieces of evidence strongly support that premature termination underlies the failure in the detection of mRNA tails.

### Supplementary Fig. 1. Premature termination of transcription.

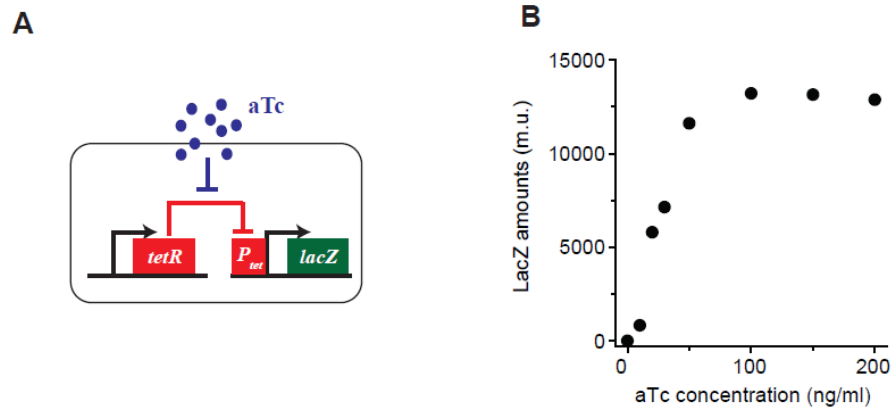


The transcription terminator factor Rho has significant effects on protein expression because it triggers premature termination of transcription<sup>29,30</sup>. But, there are other factors that influence premature termination. For example, the Nus transcription factors are involved in intrinsic termination either directly by affecting RNA structures (possibly independently of Rho) or modulating the Rho activity<sup>31-38</sup>. Gre factors stimulate transcript cleavage during transcriptional arrests, also affecting termination<sup>39,40</sup>. DksA prevents premature termination by removing transcription roadblocks<sup>41,42</sup>. A recent study revealed a role of RNAP-binding aptamers (RAPs) in premature termination<sup>43</sup>. 60% genes in *E. coli* were shown to carry RAPs. Many of these RAPs are inhibitory; they uncouple transcription and translation, marking nascent mRNAs accessible to Rho, thereby causing premature termination of transcription. The degree of premature termination varies depending on environmental conditions, which could provide a condition-dependent mechanism of gene expression.

Bicyclomycin is the selective inhibitor of Rho and has been used to identify the role of Rho in premature termination<sup>43,44</sup>. In the main text, we observed N-starved (p)ppGpp-defective cells exhibited severe defects in LacZ proteins synthesis (Fig. 3c), due to premature transcription termination (Fig. 3b). We repeated the experiment and treated (p)ppGpp-defective cells with 100  $\mu$ g/ml of bicyclomycin. The graph above shows that the treatment somewhat restored LacZ expression, although the LacZ amounts were still lower than those of N-starved wild-type cells (Fig. 3c). We performed two biologically independent experiments and obtained very similar results from the two independent experiments.

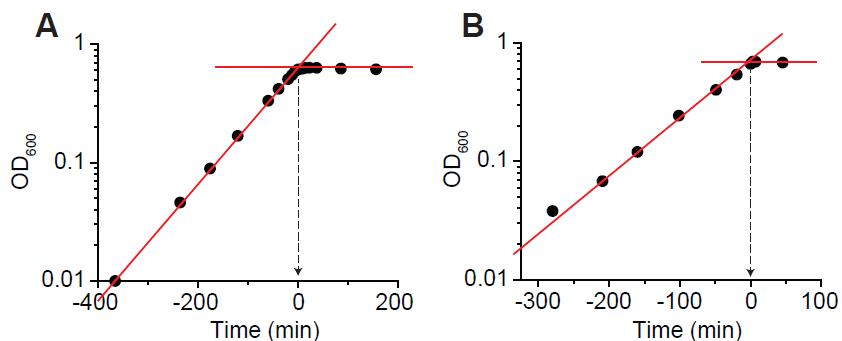
Collectively, previous studies and our results shown here indicate that Rho as well as other factors are involved in low LacZ expression of N-starved (p)ppGpp-defective cells.

**Supplementary Fig. 2. The inducer aTc fully induces LacZ expression from the P<sub>LTet-O1</sub> promoter at a concentration of 100 ng/ml.**



(A) Our strain (NMK80) harbors a synthetic promoter  $P_{LTet-O1}$  driving the expression of a *lacZ* reporter gene ( $P_{LTet-O1}$ -*lacZ*) in its chromosome<sup>1</sup>. This strain constitutively expresses TetR, a repressor of the promoter. An inducer, aTc, diffuses into cells rapidly within a couple of seconds<sup>2</sup> and relieves the repression by TetR, leading to the expression of the *lacZ* gene. (B) We added aTc to exponentially-growing cultures at various concentrations and measured the steady-state LacZ levels (we performed three biologically independent experiments and obtained very similar results from the three independent experiments). At a concentration of 100 ng/ml, LacZ expression reached the maximum, and a further increase in the concentration did not lead to higher expression. Therefore, we used 100 ng/ml of aTc in all our experiments.

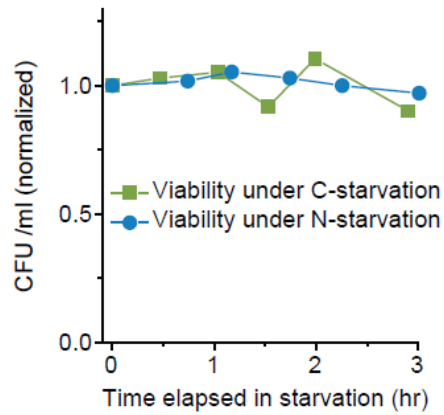
### Supplementary Fig. 3. Carbon- and nitrogen-starvation.



We cultured cells in N-C- medium<sup>45</sup>, with glycerol and ammonium as the sole carbon and nitrogen sources. For carbon starvation, we let glycerol run out by cell growth. Specifically, we supplemented medium with 6 mM glycerol and 20 mM ammonium and cultured cells in the supplemented medium. Cell growth is initially exponential and stops abruptly at  $OD_{600} \approx 0.6$  due to glycerol depletion<sup>46</sup> (panel A). This abrupt cessation of cell growth, indicating the onset of carbon starvation, defines time zero (see the arrow in panel A).  $OD_{600}$  remains constant afterwards. For nitrogen starvation, we used a low ammonium concentration and let ammonium run out by cell growth (panel B). We used 20 mM glycerol and 6 mM ammonium. Cell growth stops abruptly at  $OD_{600} \approx 0.6$ , which defines time zero (see arrow in panel B). We performed three biologically independent experiments and obtained very similar results from the three independent experiments.

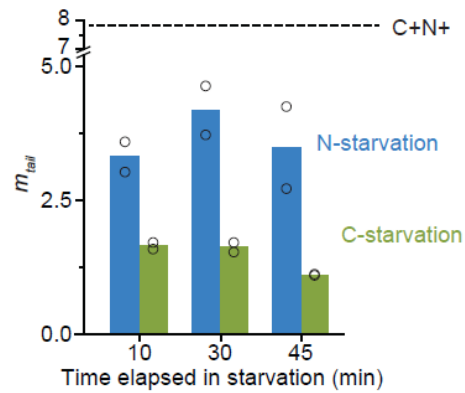
We note that glucose is a common carbon source for cell growth, being frequently used for starvation experiments (e.g., see ref.<sup>7,47</sup>). we did not use glucose in our experiments because of bacterial Crabtree effect<sup>48</sup>; cells growing on glucose excrete acetate, and the excreted acetate is used upon glucose exhaustion<sup>49</sup>. This switch to acetate upon glucose exhaustion makes it difficult to determine when starvation begins<sup>49</sup>. On the other hand, growth of cells on glycerol does not lead to acetate production<sup>50</sup>, allowing us to avoid this complication. This is why we used glycerol as the carbon source in our experiments.

**Supplementary Fig. 4. In our experimental time window, viability loss was negligible.**



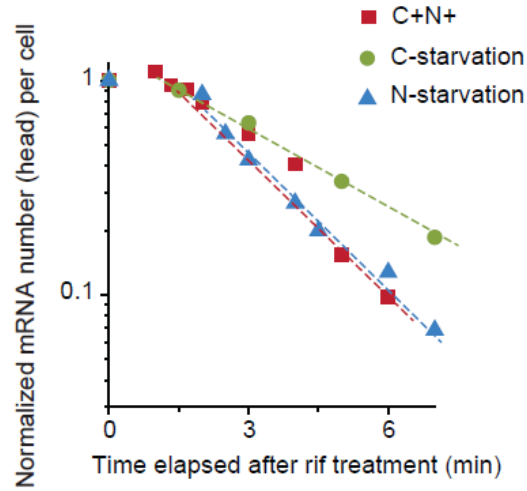
Starvation leads to gradual loss of viability<sup>8,9,46,51</sup>. As discussed in the main text, we focused on the kinetics of gene expression during the first hour of starvation. When we characterized a change in viability in starved cultures, the results showed that in our experimental time window, viability loss was negligible. We performed two biologically independent experiments and obtained very similar results from the two independent experiments.

**Supplementary Fig. 5. Comparing the average copy number of mRNA tail per cell,  $m_{tail}$ , in C+N+, C-starved, and N-starved cells.**



The average copy number of mRNA tail per cell,  $m_{tail}$  was plotted here (the average copy number of mRNA head per cell,  $m_{head}$ , was plotted in Fig. 1b). Starvation led to a significant reduction in mRNA amount; see blue columns on the left for N-starvation and green columns on the right for C-starvation. The reduction was more severe under C-starvation than N-starvation. Two biologically independent experiments were performed. The dots and bar show the data from the two independent experiments and their mean.

**Supplementary Fig. 6. Characterizing mRNA degradation kinetics.**



The mRNA amounts are determined by the mRNA synthesis rate,  $\alpha_m$ , and the degradation rate,  $\beta_m$  in the following manner,

$$\frac{dm}{dt} = \alpha_m - \beta_m \cdot m . \quad \text{Eq. (S1)}$$

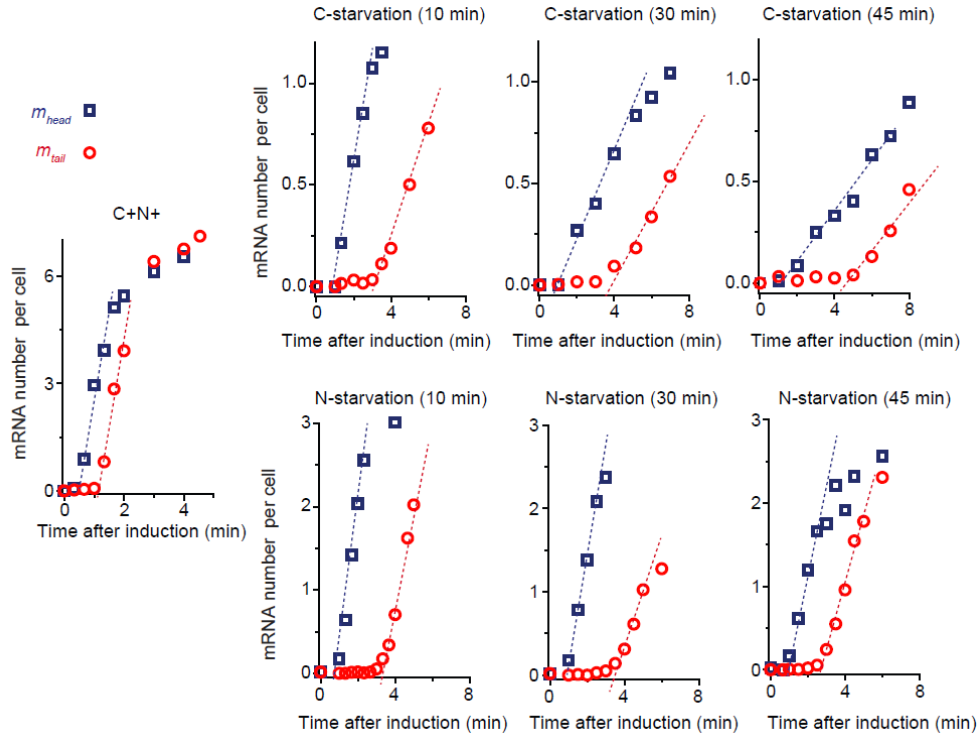
Consider that *lacZ* expression was induced previously, and then at time zero, the induction was inhibited abruptly, e.g., by adding a transcription inhibitor, rifampicin (rif) to the culture. From then on, the mRNA synthesis rate would be zero. Applying  $\alpha_m = 0$  to the Eq. (S1) in the main text, i.e., the law of mass action for transcriptional kinetics, we have

$$m(t) = m(0) \exp(-\beta_m \cdot t) , \quad \text{Eq. (S2)}$$

where  $m$  is the mRNA amount at a given time  $t$ . Eq. (S2) predicts that after the inhibition of mRNA synthesis,  $m$  decreases exponentially over time, and the rate of a decrease is equal to the degradation rate  $\beta_m$ .

In our experiments, we induced mRNA *lacZ* mRNA synthesis using 100 ng/ml of aTc for 10 mins and then inhibited the synthesis using rifampicin (the inhibition defined time zero). As predicted, mRNA amounts decreased exponentially; see a linear decrease in the semi-log plots above for exponentially growing cells in a nutrient-rich condition (red squares), cells starved of carbon for 30 mins (green circles) and cells starved of nitrogen for 30 mins (blue triangles). Analyzing the slopes, we determined the degradation rate  $\beta_m$ . We repeated this procedure for cells starved for different duration and reported the values of  $\beta_m$  in Supplementary Table 1. In all cases, two biologically independent experiments were performed. We obtained very similar results from the two independent experiments.

**Supplementary Fig. 7. Characterizing the induction kinetics of *lacZ* mRNA.**



We determined the *lacZ* mRNA synthesis rate under C+N+ (the left plot), C-starvation (top panel), and N-starvation (bottom panel) conditions, by characterizing how mRNA amounts increased after induction. First, aTc was added to an exponentially-growing culture in the C+N+ condition at a final concentration of 100 ng/ml; the addition defined time zero. We observed that the amounts of the mRNA head ( $m_{head}$ , blue squares) and tail ( $m_{tail}$ , red circles) increased linearly (the left plot). When we prepared cells starved of carbon (top panel) and nitrogen (bottom panel) and add aTc to the cultures at different times, we again observed linear increases of  $m_{head}$  and  $m_{tail}$ , although the slopes were different.

This linear increase can be understood using Eq. (S1), i.e., the law of mass action for transcriptional kinetics. Immediately after the induction of mRNA expression, the mRNA amounts are very low, and Eq.

(S1) can be approximated by  $\frac{dm}{dt} = \alpha_m$ . Assuming  $\alpha_m$  does not change much during the short period of measurements (a few minutes as shown above), we have

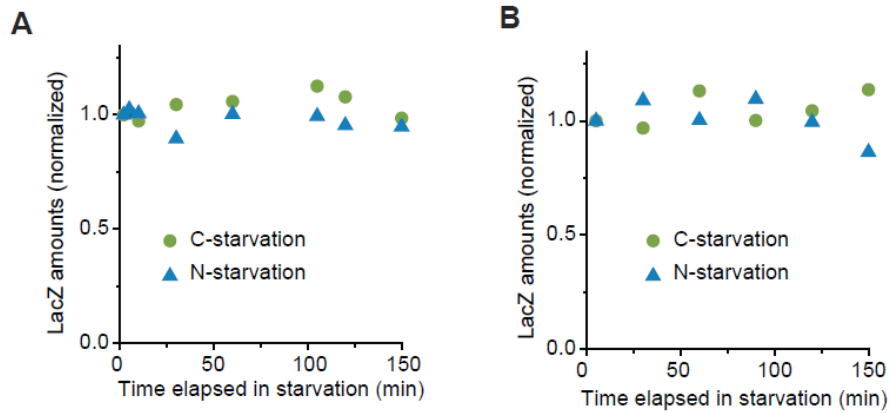
$$m = \alpha_m \cdot t \quad \text{Eq. (S3)}$$

Thus, soon after induction, mRNA amounts increase linearly and the slope of the linear increase is equal to the mRNA synthesis rate,  $\alpha_m$ . The values of  $\alpha_m$  determined in this manner were reported in Fig. 1c and Supplementary Table 1.

Additionally, the data plotted above were used to calculate mRNA-chain elongation speeds; see our recently published article for details <sup>2</sup>. Briefly, after promoter induction, the head of the mRNA appeared with a time delay (blue squares). The X-intercept of the fit (blue lines) reflects the delay and we denote the X-intercept by  $T_{head}$ . With the knowledge of the length of the head (Fig. 1a and Supplementary Table 4 and 5), the time delay was used to calculate the mRNA-chain elongation speed (Method A). Please note that we considered the time delay between the addition of the inducer to the medium and transcription initiation, which we denoted as  $T_{lag}$ ; we showed that  $T_{lag}$  is 6.5 sec in our previous study <sup>2</sup>. Therefore, the transcription elongation speed is equal to  $935 \text{ nt} / (T_{head} - 6.5 \text{ sec})$ . Alternatively, the time delay between the appearance of the head (blue squares) and the appearance of the tail (red circles) can be used to calculate the speed (Method B); the transcription elongation speed would be  $(3075 \text{ nt} - 935 \text{ nt}) / (T_{tail} - T_{head})$ . We previously showed that the speeds calculated from these two different methods are consistent <sup>2</sup>. We further tested the consistency of the two methods by using the data plotted here for C+N+ cells, cells starved of carbon for 45 mins, and cells starved of nitrogen for 45 mins. Using Method A and B respectively, we obtained  $48.6 (\pm 2.2)$  and  $49.0 (\pm 3.7)$  nt/sec in C+N+ cells,  $12.9 (\pm 2.5)$  and  $12.7 (\pm 2.1)$  nt/sec in C-starved cells, and  $20.9 (\pm 3.2)$  and  $19.7 (\pm 1.2)$  nt/sec in N-starved cells (here, we reported the mean and standard deviation of values obtained from two independent experiments). These results show that the two methods yield consistent results. Throughout this work, we determined the speed from the time of appearance of the head signals (Method A), because in some experiments, there are no tail signals due to premature termination (e.g., see Fig. 3b). In all cases, two biologically independent experiments were performed. We obtained very similar results from the two independent experiments.

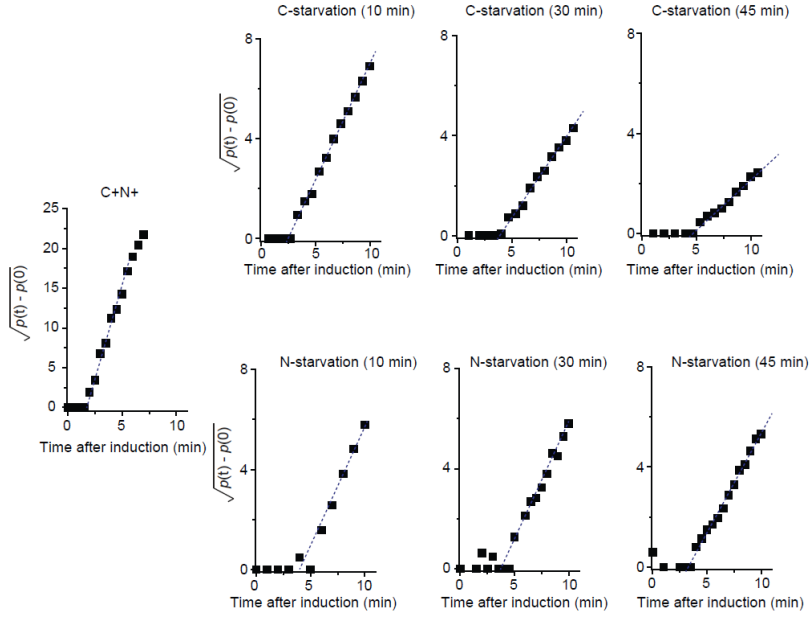
In the main text, we discussed that C-starvation has severe effects on transcription. For example, when cells were starved of carbon for 45 mins, the transcription rate decreased more than 10 fold, whereas the transcription elongation speed decreased ~2.5 fold (the actual values of these rates and speeds were provided in the main text and Fig. 1c). A much greater decrease in the transcription rate compared to the transcription elongation speed indicates that transcription initiation is rate-limiting in transcription during C-starvation.

**Supplementary Fig. 8. LacZ proteins were not degraded in our experimental time window.**



We measured the LacZ degradation rate,  $\beta_p$  in two different experiments. **(A)** We first induced LacZ expression using aTc, and then stopped the expression by suspending cells in inducer-free medium. We observed that protein levels remained constant in N-starved cells, as well as C-starved cells. **(B)** In a separate experiment, we stopped protein synthesis using chloramphenicol, the translation elongation inhibitor. Again, the protein levels remained constant. Therefore, LacZ proteins were not degraded in starved cells, i.e.,  $\beta_p = 0$ . In all cases, two biologically independent experiments were performed. We obtained very similar results from the two independent experiments.

## Supplementary Fig. 9. Characterizing the kinetics of LacZ protein expression



The LacZ amount,  $p$ , is governed by the number of mRNA molecules ( $m$ ), rate of protein synthesis from a single mRNA molecule ( $\alpha_p$ ), and rate of protein degradation ( $\beta_p$ ), in the following manner,

$$\frac{dp}{dt} = m \cdot \alpha_p - \beta_p \cdot p \quad \text{Eq. (S4)}$$

In Supplementary Fig. 8, we showed that the rate of protein degradation is zero ( $\beta_p = 0$ ). Thus, we have

$$\frac{dp}{dt} = m \cdot \alpha_p \quad \text{Eq. (S5)}$$

In Supplementary Fig. 7, we established that immediately after induction, *lacZ* mRNA amount increases linearly; see Eq. (S3). Combining Eq. (S3) and Eq. (S5), we have

$$\frac{dp}{dt} = \alpha_m \cdot \alpha_p \cdot t \quad \text{Eq. (S6)}$$

Taking the integral, we have

$$\sqrt{p(t) - p(0)} = \sqrt{\frac{\alpha_m \cdot \alpha_p}{2}} \cdot t, \quad \text{Eq. (S7)}$$

where  $p(0)$  is the amount of LacZ proteins present before induction, due to its leaky basal expression. Thus, immediately after induction, the square root of LacZ amounts increases linearly against time, and the plots above confirmed this prediction. Importantly, the slope of the linear increase is determined by

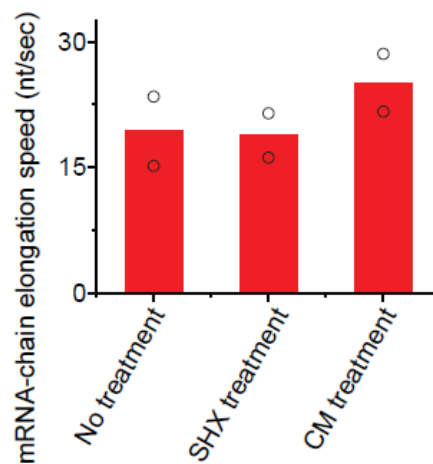
the mRNA synthesis rate,  $\alpha_m$ , and protein synthesis rate,  $\alpha_p$  (Eq. (S7)). Analyzing the slope, and using the value of  $\alpha_m$  that we previously determined (Supplementary Fig. 7 and Supplementary Table 1), we calculated  $\alpha_p$  (Fig. 1e). Note that we have used  $\alpha_m$  from the mRNA tail because it reflects the synthesis rate of full-length mRNAs. In all cases, two biologically independent experiments were performed. We obtained very similar results from the two independent experiments.

Previous studies routinely determined the peptide-chain elongation speed using a time delay in the appearance of the LacZ protein after induction<sup>52-56</sup>. Such a delay is evident in our data shown here, which we used to determine the peptide-chain elongation speed under starvation conditions.

In summary, translation rates and translation elongation speeds can be separately determined by measuring the slopes and delays in the appearance of LacZ amounts.

Previous studies showed that starvation leads to a decrease in ATP and GTP levels, although the decrease is minor during the first hour of starvation (which was the focus of our study)<sup>24,57,58</sup>. Such a decrease is expected to contribute to changes in transcription and translation processes observed in our study.

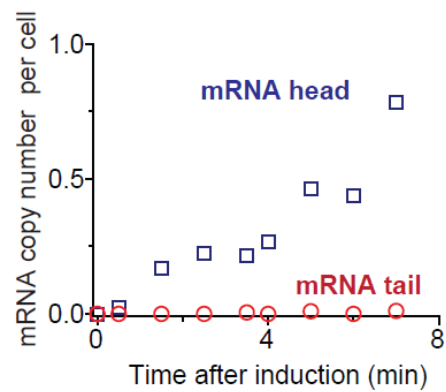
**Supplementary Fig. 10. Transcription elongation speed in N-starved cells treated with serine hydroxamate (SHX) or chloramphenicol (CM) or without any treatment.**



In our experiments, chloramphenicol treatment was used to show that translation inhibition does not slow down transcription elongation under nitrogen starvation (Fig. 2c). Previous studies have shown that chloramphenicol treatment results in a decrease in (p)ppGpp levels<sup>25-27</sup>, which could possibly complicate the interpretation of the results. To test this possibility, we repeated the experiments using serine hydroxamate (SHX). SHX prevents charging of seryl-tRNAs and leads to ribosome stalling, hence inhibiting translation like chloramphenicol<sup>59</sup>. However, unlike chloramphenicol, SHX induces (p)ppGpp synthesis, leading to an increase in (p)ppGpp levels<sup>60</sup>. When we treated cells starved of nitrogen for 10 mins with SHX, we found the transcription elongation speed is very similar to the speed without any treatment (see the panel above), again demonstrating that translation inhibition does not slow down transcription elongation even when (p)ppGpp synthesis is induced. We note that the transcription elongation speed with chloramphenicol treatment is somewhat higher, possibly due to the negative effects of chloramphenicol on (p)ppGpp concentrations<sup>25-27</sup>. In any case, the control experiment with SHX indicates that the interpretation of our results (i.e., that translation inhibition does not slow down transcription elongation under nitrogen starvation) holds true and is not complicated by the negative effect of chloramphenicol on (p)ppGpp concentrations. In all cases, two biologically independent experiments were performed. The dots and bar show the data from the two independent experiments and their mean.

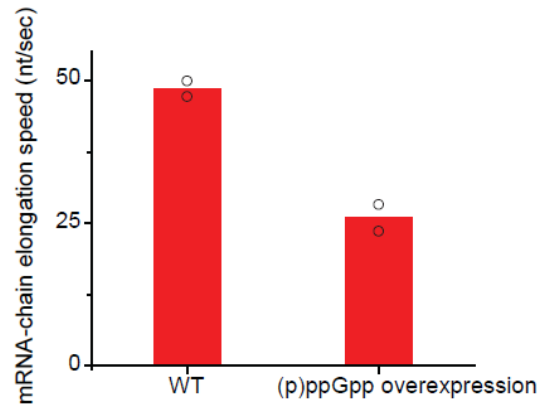
Currently, the kinetic process responsible for (p)ppGpp-mediated coordination of transcription and translation under N-starvation is unclear. One possible mechanism, which is supported by the match of transcription elongation speeds with and without SHX treatment as shown above, is that (p)ppGpp slows down RNAPs, and ribosomes catches up with RNAPs and slow down accordingly.

**Supplementary Fig. 11. The kinetics of *lacZ* mRNA expression under C+N+ with chloramphenicol treatment.**



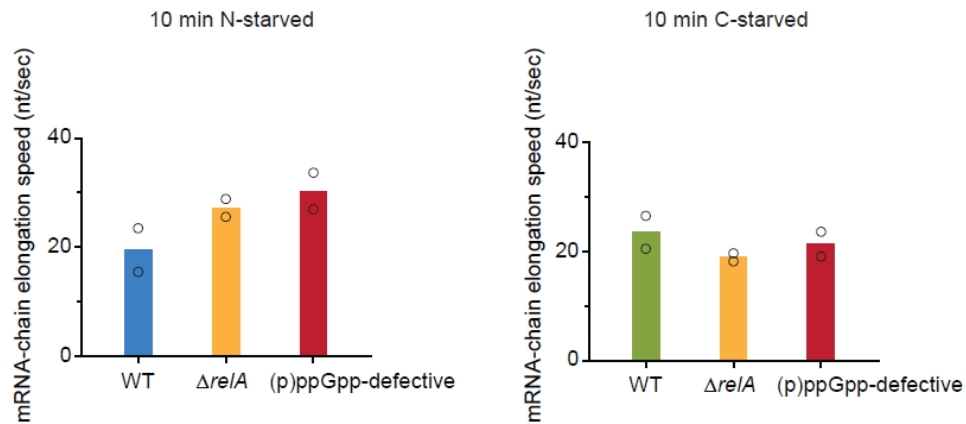
We cultured cells in nutrient-rich conditions and added chloramphenicol (100  $\mu\text{g/ml}$ ). After 5 minutes of incubation, we added aTc (100 ng/ml). The chloramphenicol abolished the synthesis of the mRNA tails. Two biologically independent experiments were performed. We obtained very similar results from the two independent experiments.

**Supplementary Fig. 12. (p)ppGpp accumulation results in a lower transcription elongation speed.**



In *E. coli*, (p)ppGpp molecules are synthesized by two enzymes, mono-functional RelA (with synthesis activity only) and bi-functional SpoT (with synthesis and hydrolysis activities) <sup>61</sup>. In WT cells under nutrient-rich conditions, (p)ppGpp levels are very low, because both the expression of these enzymes and their activities are low <sup>62,63</sup>. To increase the (p)ppGpp concentration, we utilized a plasmid containing  $P_{tac}$ -*relA'*, pALS13 <sup>3</sup>. The *relA'* is a truncated *relA* gene and encodes a catalytically active protein containing the first 455 amino acids of the RelA protein. In contrast to native RelA, the RelA' protein maintains strong synthesis activity even in nutrient-rich conditions. Its expression, driven by the promoter  $P_{tac}$ , can be controlled artificially using the inducer IPTG. We introduced this plasmid into our *E. coli* strain, cultured the resulting strain (NMK156) in C+N+ minimal medium, and stimulated (p)ppGpp synthesis by adding 1 mM IPTG. The synthesis led to a reduction in the transcription elongation speed by ~2-fold. In all cases, two biologically independent experiments were performed. The dots and bar show the data from the two independent experiments and their mean.

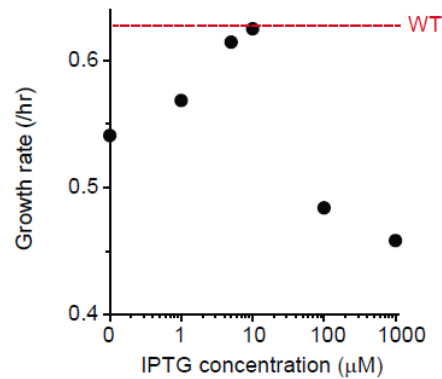
**Supplementary Fig. 13. Comparing the transcription elongation speed for 10 mins-starved cells.**



We compared the mRNA-chain elongation speed of the (p)ppGpp-defective strain to that of the WT strain subjected to the same C-starvation condition. The data for 30 min starvation were shown in Fig. 3a and 3d. Here, we reported the speeds for 10 mins-starved cells. In all cases, two biologically independent experiments were performed. The dots and bar show the data from the two independent experiments and their mean.

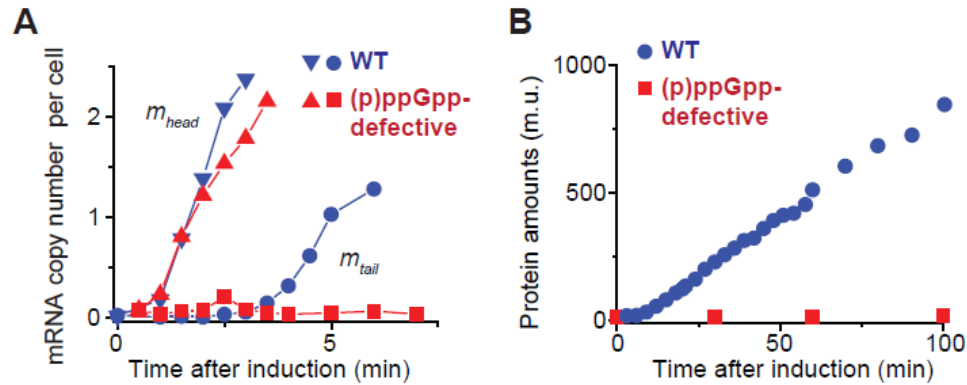
We found that (p)ppGpp synthesis defect did not lead to an increase in the speed under C-starvation (Fig. 3d and panel B here). This lack of increase under C-starvation may also be accounted for by the translation-aid-transcription mechanism. As discussed in the main text, when RNAPs transcribe a DNA template, in the absence of trailing ribosomes, they frequently pause and backtrack<sup>64-66</sup>. Roadblocks along a DNA template (e.g., DNA-bound molecules) exacerbate this pausing and backtracking, further slowing down transcription elongation<sup>55</sup>. However, translational motion of ribosomes is highly energetic and processive<sup>67</sup>. Thus, with the translation-aid-transcription mechanism, trailing ribosomes help RNAPs push away the roadblocks<sup>55</sup>. It is possible that a similar process is in play; the translation-aid-transcription mechanism helps to overcome the repressive effect of (p)ppGpp on transcription elongation under C-starvation. Importantly, the translation-aid-transcription mechanism is no longer in effect under N-starvation. Therefore, the repressive effect of (p)ppGpp is expected to be evident. Indeed, the (p)ppGpp synthesis defect leads to a significant increase in transcription elongation speed (Fig. 3a and panel A here).

**Supplementary Fig. 14. The growth rate of the (p)ppGpp-defective strain in C+N+ minimal media.**



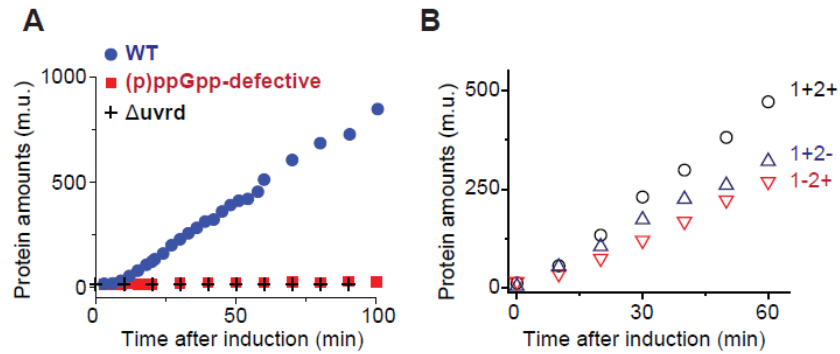
We constructed a strain that is capable of producing (p)ppGpp at a low level and yet incapable of accumulating it in massive amounts under starvation (NMK217). First, to abolish the rapid accumulation of (p)ppGpp upon starvation, we replaced the native  $P_{\text{relA}}\text{-relA}$  on the chromosome in WT cells (NMK80) with  $P_{\text{tac}}\text{-relA}'$  (cloned from pALS13<sup>3</sup>). Also, the native *spoT* gene was replaced by *spoT-E319Q*, which contains a mutation that eliminated (p)ppGpp synthesis<sup>4</sup>. In the resulting strain (NMK217), (p)ppGpp synthesis can be artificially controlled using the  $P_{\text{tac}}$  inducer IPTG. When we cultured this strain in C+N+ minimal medium (containing glycerol and ammonium as the sole carbon and nitrogen sources), with 10  $\mu\text{M}$  IPTG, it grew at the same rate as WT; see the plot above. Above and below this concentration, this strain exhibited growth defects; this observation agrees with previous reports that non-optimal (p)ppGpp levels resulted in defective growth<sup>3,68,69</sup>. This growth pattern indicates that in C+N+ minimal medium, with 10  $\mu\text{M}$  IPTG, this strain maintained a basal (p)ppGpp level comparable to that of WT cells. Thus, throughout the experiment, we maintained the level of IPTG at 10  $\mu\text{M}$  in the culture. Two biologically independent experiments were performed. We obtained very similar results from the two independent experiments.

**Supplementary Fig. 15. Premature transcription termination in the (p)ppGpp-defective strain.**



In the main text, we cultured the (p)ppGpp-defective strain with 10  $\mu$ M IPTG. Under N-starvation, this strain produced the mRNA heads similarly to WT cells but failed to produce mRNA tails (Fig. 3b), and failed to produce LacZ proteins (Fig. 3c). We repeated this experiment with no IPTG. This strain again produced the mRNA heads similarly to WT cells but failed to produce mRNA tails (panel A), and failed to produce LacZ proteins (panel B). Our observation remained the same when we repeated the experiments with 20  $\mu$ M IPTG. Therefore, our observation of premature termination and failure to produce LacZ proteins does not depend on the exact (p)ppGpp concentrations. In all cases, two biologically independent experiments were performed. We obtained very similar results from the two independent experiments.

**Supplementary Fig. 16. (p)ppGpp is likely to act directly on RNA polymerases.**

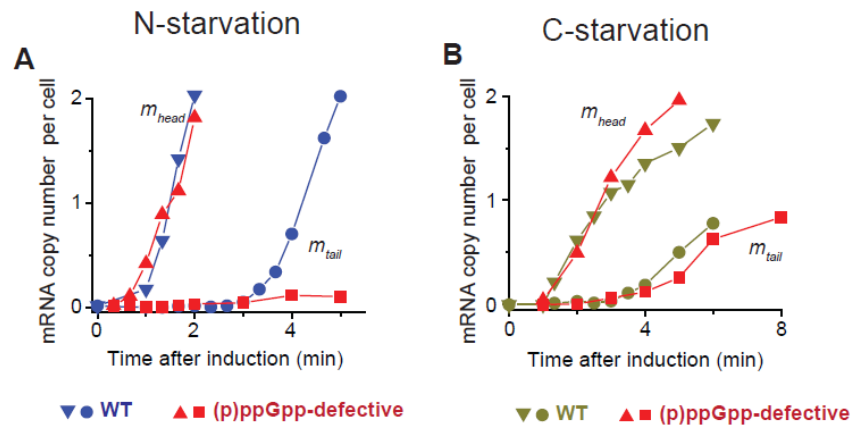


Upon starvation, (p)ppGpp level increases during the first 10 mins<sup>22-24,70,71</sup>. We found that (p)ppGpp slows down transcriptional elongation (Fig. 3 and Supplementary Fig. 12 and 13). This slow-down is critical for gene expression under N-starvation, as the (p)ppGpp-defective strain, which exhibited fast transcriptional elongation, was not able to express LacZ proteins (and also other proteins); see Fig. 3c and 4a.

In our data, the slow-down of transcriptional elongation by (p)ppGpp is already evident at 10 mins after N-starvation (Supplementary Fig. 13). This rapid response supports the possibility that (p)ppGpp directly acts on RNAPs. Previous studies have shown that UvrD binds to RNA polymerases (RNAP) and promotes RNAP backtracking<sup>72,73</sup>. To test the role of UvrD in our findings, we repeated the LacZ measurements under N-starvation using the  $\Delta uvrD$  strain. In Fig. 3c, we showed that under N-starvation, the WT strain expresses LacZ proteins while the (p)ppGpp-defective strain exhibits severe defects in LacZ protein synthesis; these data are re-plotted in the panel A above. When we repeated the experiments using the  $\Delta uvrD$  strain, we found that the  $\Delta uvrD$  strain also exhibits severe defects in LacZ protein synthesis (panel A). This finding suggests that UvrD is involved, possibly mediating the binding of (p)ppGpp on RNAPs during transcriptional elongation slow-down. Please note that the experiments with the  $\Delta uvrD$  strain had to be repeated multiple times because this strain exhibits increased spontaneous mutagenesis<sup>74</sup>; we found that when this strain was cultured for extended periods of time, the strain expressed LacZ proteins under N-starvation. Furthermore, recent biochemical studies showed that (p)ppGpp can directly bind to RNAPs, forming a transcription complex<sup>75-77</sup>. Two binding sites were identified and strains lacking these sites were constructed<sup>76</sup>. We received these strains, RLG14535 (both binding sites intact, 1+2+), RLG14536 (the first binding site is deleted, 1-2+), and RLG14537 (the second binding site is deleted, 1+2-). We starved them of nitrogen and artificially expressed LacZ proteins from the native promoter by adding 1 mM of IPTG and 10 mM of cAMP. We observed that the strains lacking binding sites exhibited defects in LacZ protein synthesis (panel B). In all cases two biologically

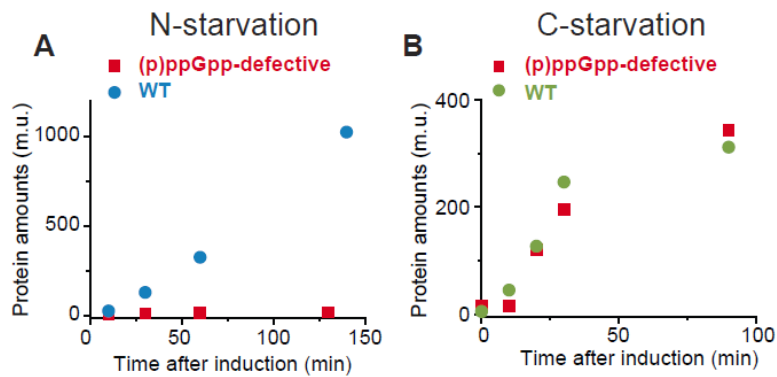
independent experiments were performed. We obtained very similar results from the two independent experiments.

**Supplementary Fig. 17. Comparing the kinetics of mRNA synthesis for 10 min-starved WT and (p)ppGpp-defective strains.**



In the main text, we reported mRNA synthesis kinetics for WT and (p)ppGpp-defective strains starved of carbon or nitrogen for 30 mins (Fig. 3b and 3e). Here, we reported the kinetics for 10 mins-starved cells. In all cases, two biologically independent experiments were performed. We obtained very similar results from the two independent experiments.

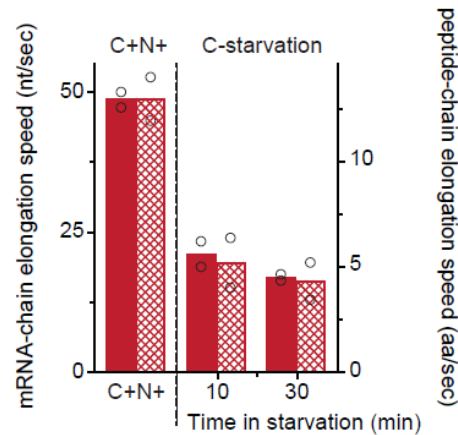
**Supplementary Fig. 18. Comparing the kinetics of LacZ protein synthesis for 10 min-starved WT and (p)ppGpp-defective strains.**



In the main text, we reported the kinetics of LacZ protein synthesis for WT and (p)ppGpp-defective strains starved of carbon or nitrogen for 30 mins (Fig. 3c and 3f). Here, we reported the kinetics for 10 mins-starved cells. In all cases, two biologically independent experiments were performed. We obtained very similar results from the two independent experiments.

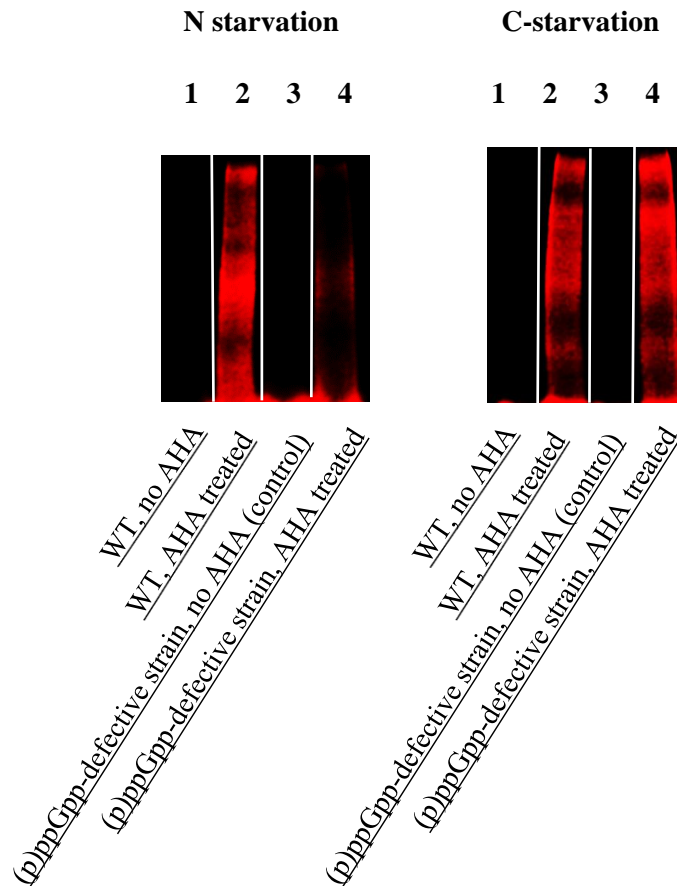
**Supplementary Fig. 19. Comparing the transcription and translation elongation speeds for the (p)ppGpp-defective strain.**

Comparison of transcription elongation (left axis; solid) and translation elongation (right axis; stripe)



In Fig. 2d, we plotted *lacZ* mRNA-chain elongation speed (a red solid column, left axis) and LacZ peptide-chain elongation speed (a red striped column, right axis) in WT cells under the C+N+ condition. The scales of the axes were adjusted such that the heights of the two columns matched. We re-plotted them in the same manner here on the left. To the right, we then plotted the mRNA-chain elongation speed of the (p)ppGpp-defective strain starved of carbon (left axis, solid), which showed that the speed was lower than that of the WT strain in the C+N+ condition. Next to them, we plotted the peptide-chain elongation speed of the same strain under the same condition as red striped columns (right axis). The heights of these columns remained matched, indicating that the peptide-chain elongation speed decreased by the same degree as the mRNA-chain elongation speed. In all cases, two biologically independent experiments were performed. The dots and bar show the data from the two independent experiments and their mean.

**Supplementary Fig. 20. Characterizing global protein synthesis activity during starvation for the WT and (p)ppGpp-defective strains.**

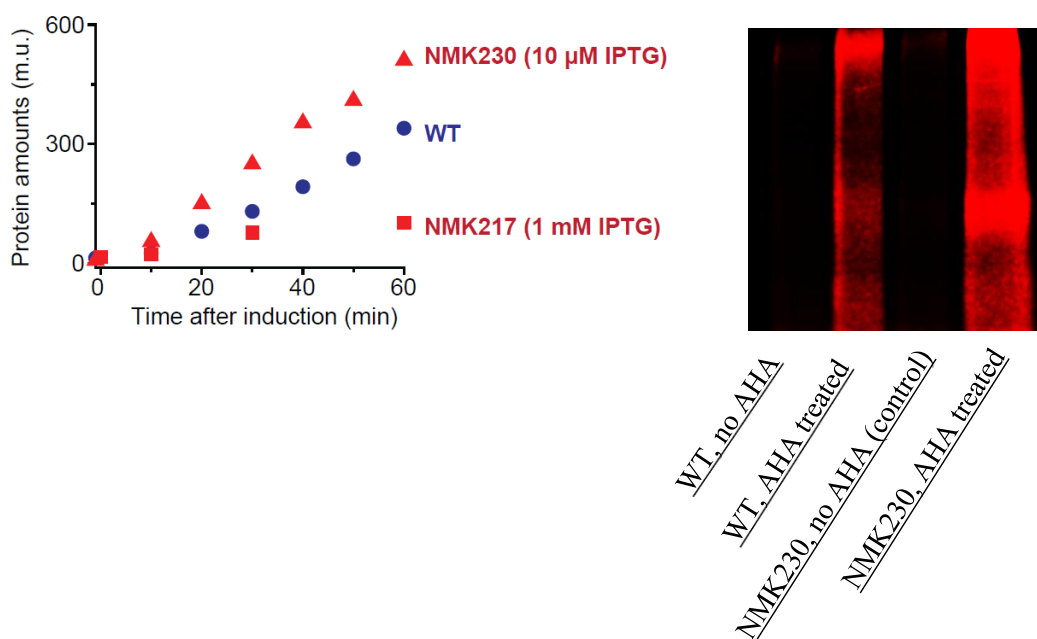


Starvation leads to up-regulated expression of hundreds of proteins<sup>15,78</sup>. To compare total protein synthesis activities between WT and (p)ppGpp-defective strains, we fluorescently labeled proteins newly synthesized during starvation and compared the total fluorescence intensities<sup>79-81</sup>; See text. We first starved WT and (p)ppGpp-defective cells of nitrogen at time zero, and immediately added *L*-azidohomoalanine (AHA), the amino acid surrogate for *L*-methionine, to the culture. AHA, replacing methionine, is incorporated into proteins synthesized during starvation. After 1 hour, we collected cells and fluorescently labeled the AHA molecules incorporated into the proteins (see Methods for detail). Here we showed raw images of the fluorescent protein gel. Even from a cursory visual inspection, it is clear that the fluorescence intensity for the WT strain (the left image, the second lane) is much higher than that for the (p)ppGpp-defective strain (the left image, the fourth lane). We measured the total fluorescence intensities and reported their relative values in Fig. 4a.

We repeated this procedure using cells starved of carbon. In contrast to our observation under N-starvation, the fluorescence intensity for the WT strain (the right image, the second lane) is about the

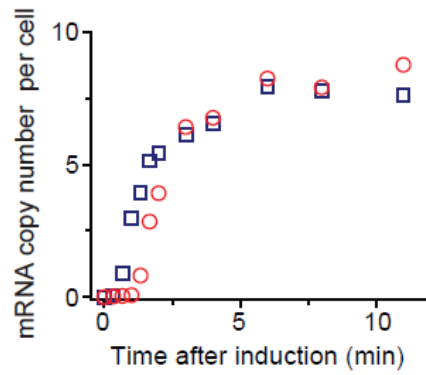
same as that for the (p)ppGpp-defective strain (the right image, the fourth lane). We measured the total fluorescence intensities and reported the values in Fig. 4b. Two biologically independent experiments were performed. We obtained very similar results from the two independent experiments.

**Supplementary Fig. 21. Characterizing global protein synthesis activity with *relA'* overexpression**



By starving NMK217 of nitrogen, we showed that ppGpp synthesis defect leads to inhibition of LacZ expression and global protein synthesis (Fig. 4a and Supplementary Fig. 20). Here, we characterized the effect of (p)ppGpp over-synthesis. NMK217 harbors  $P_{tac}$ -*relA'* on the chromosome. When we induced *relA'* expression with 10 μM IPTG, this strain failed to produce LacZ proteins (Fig. 4c). When we induced the expression with 1 mM IPTG, LacZ expression in this strain was lower than that in WT; compare the blue circles and red squares in the left panel above. We then induced the *relA'* expression from a plasmid pALS13 containing  $P_{tac}$ -*relA'*; see the ref. <sup>3</sup> for details of this plasmid and see NMK230 in Supplementary Table 2 for details of the strain used. We found that with 10 μM IPTG, NMK230 expressed higher amounts of LacZ proteins than WT; compare the blue circles and red triangles in the left panel above. We then followed the procedure described in Supplementary Fig. 20 and measured the total protein synthesis activities. Even from a cursory visual inspection of raw images of the fluorescent protein gel (right panel), it is clear that NMK230 exhibits higher global protein synthesis activities than WT; compare the second and fourth lanes. Two biologically independent experiments were performed. We obtained very similar results from the two independent experiments.

**Supplementary Fig. 22. The kinetics of *lacZ* mRNA expression under C+N+.**



We determined the *lacZ* mRNA amounts after induction under C+N+. aTc was added to an exponentially-growing culture in the C+N+ condition at a final concentration of 100 ng/ml; the addition defined time zero. We observed that the amounts of the mRNA head ( $m_{head}$ , blue squares) and tail ( $m_{tail}$ , red circles) increase, reaching their steady state levels within 5 mins. Two biologically independent experiments were performed. We obtained very similar results from the two independent experiments.

**Supplementary Table 1. Values of all the data obtained from this study.**

	C+N+	Carbon-starved			Nitrogen-starved		
		10 mins	30 mins	45 mins	10 mins	30 mins	45 mins
lacZ mRNA head copy number	7.6	1.9	1.6	1.2	4.7	3.7	3.2
lacZ mRNA tail copy number	7.9	1.6	1.6	1.1	3.3	4.2	3.5
LacZ protein amounts (m.u.)	12705	127.0	246.8	300.0	47.6	150.3	250.1
lacZ mRNA head synthesis rate (/min)	5.3	0.4	0.2	0.1	1.9	1.3	1.0
lacZ mRNA tail synthesis rate (/min)	5.3	0.3	0.1	0.1	1.2	0.7	0.8
LacZ protein synthesis rate (m.u./min)	8.7	5.1	4.4	4.1	1.2	1.9	1.3
lacZ mRNA-chain elongation speed (nt/sec)	48.6	23.3	16.9	12.9	19.3	20.4	20.9
LacZ peptide-chain elongation speed (aa/sec)	12.9	5.7	4.6	3.5	4.1	5.2	5.3
lacZ mRNA head degradation rate (/min)	-0.49	-0.23	-0.24	-0.15	-0.53	-0.52	-0.56
lacZ mRNA tail degradation rate (/min)	-0.52	-0.22	-0.25	-0.16	-0.55	-0.5	-0.58
lacZ mRNA-chain elongation speed, chloramphenicol treated. (nt/sec)	22.3	15.9	6.4	4.6	25.1	22.2	19.4
lacZ mRNA-chain elongation speed, (p)ppGpp overexpression using pALS13 (nt/sec)	26.0						
lacZ mRNA-chain elongation speed, relA deletion (nt/sec)		18.7	17.3		27.0	23.5	21.9
lacZ mRNA-chain elongation speed, (p)ppGpp-defective strain (nt/sec)		21.1	16.9		30.1	35.0	
LacZ peptide-chain elongation speed, (p)ppGpp-defective strain (aa/sec)		5.2	4.3				

**Supplementary Table 2. Strain list**

Strain	Genotype	Derived from	Comments	Reference
NCM3722	-	-	<i>E. coli</i> K-12 wild-type strain	82-84
NMK 80	P <sub>lacZ-rbs</sub> ::P <sub>tet-rbs1</sub> , ΔlacI, sp:P <sub>con</sub> -TetR-LacIq(attB)	NCM3722		2
NMK 156	P <sub>lacZ-rbs</sub> :P <sub>tet-rbs1</sub> , ΔlacI, sp:P <sub>con</sub> -TetR-LacIq(attB); PLASMID: pALS13	NMK 80	NMK80 was transformed with the pALS13 plasmid	See <sup>3</sup> for pALS13
NMK 210	P <sub>lacZ-rbs</sub> ::P <sub>tet-rbs1</sub> , ΔlacI, sp:P <sub>con</sub> -TetR-LacIq(attB), p <sub>relA-relA</sub> ::p <sub>tac-relA'</sub> :km	NMK 80	p <sub>tac-relA'</sub> in the pALS13 plasmid was PCR-amplified and fused to kanamycin cassette from pKD13. This fusion product replaced the native p <sub>relA-relA</sub> in NMK80.	See <sup>6</sup> for pKD13
NMK 215	P <sub>lacZ-rbs</sub> ::P <sub>tet-rbs1</sub> , ΔlacI, sp:P <sub>con</sub> -TetR-LacIq(attB), spoT E319Q zib563::Tn10	NMK 80	Performed P1 transduction to move the spoT E319Q zib563::Tn10 allele into NMK 80.	See <sup>4</sup> for spoT E319Q allele
NMK 217	P <sub>lacZ-rbs</sub> ::P <sub>tet-rbs1</sub> , ΔlacI, sp:P <sub>con</sub> -TetR-LacIq(attB), p <sub>relA-relA</sub> ::p <sub>tac-relA'</sub> :km, spoT E319Q zib563::Tn10	NMK 215	Performed P1 transduction to move the p <sub>tac-relA'</sub> :km allele from NMK 210 into NMK 215	
NMK 230	P <sub>lacZ-rbs</sub> ::P <sub>tet-rbs1</sub> , ΔlacI, sp:P <sub>con</sub> -TetR-LacIq(attB), ΔrelA, spoT E319Q zib563::Tn10, PLASMID: pALS13			

**Supplementary Table 3. Primer list**

Primer Name	Primer sequence
ins_tac_relA_fwd	ttgtcgacgtcaacaatgc
tac_relA_fwd	ttgtcgacgtcaacaatgccccatttagcgccccaactgaagcattggcataattcggtcgtcctcaa
relA_kan_rev	ggaactcgaactgcaggtcgagccaggcaattctgtttatc
kan_relA_rev	gattgagcgctgcattaactagccgggatccgcaccgctgaatttgctgcttcaagttcctataC

ins\_relA\_rev

gattgagcgcctgcattaac

**Supplementary Table 4. Sequence of the *lacZ* gene, with the probe-binding sequences underlined**

ATGACCATGATTACGGATTCACTGGCCGTCGTTTTACAACGTCGCTGACTGGGAAAACCCTGG  
CGTTACCCAACTTAATCGCCTTGCAGCACATCCCCCTTTCGCCAGCTGGCGTAATAGCGAAG  
AGGCCCGCACCGATCGCCCTTCCCAACAGTTGCGCAGCCTGAATGGCGAATGGCGCTTTGCC  
TGGTTTTCCGGCACCAGAAGCGGTGCCGAAAGCTGGCTGGAGTGCGATCTTCTGAGGCCG  
ATACTGTCGTCGTCCCCTCAAACTGGCAGATGCACGGTTACGATGCGCCCATCTACACCAAC  
GTGACCTATCCCATTACGGTCAATCCGCCGTTTGTTCCCACGGAGAATCCGACGGGTTGTTA  
CTCGCTCACATTTAATGTTGATGAAAGCTGGCTACAGGAAAGGCCAGACGCGAATTATTTTTG  
ATGGCGTTAACTCGGCCTTTCATCTGTGGTGCACCGGGCGCTGGGTTCGGTTACGGCCAGGAC  
AGTCGTTTGCCGTCTGAATTTGACCTGAGCGCATTTTTACGCGCCGGAGAAAACCGCCTCGC  
GGTGATGGTGCTGCGCTGGAGTGACGGCAGTTATCTGGAAGATCAGGATATGTGGCGGATG  
AGCGGCATTTTCCGTGACGTCTCGTTGCTGCATAAACCGACTACACAAATCAGCGATTTCCA  
TGTTGCCACTCGCTTTAATGATGATTTACGCCGCGCTGACTGGAGGCTGAAGTTCAGATGT  
GCGGGCAGTTGCGTGACTACCTACGGGTAACAGTTTCTTTATGGCAGGGTGAAACGCAGGTC  
GCCAGCGGCACCGCGCCTTTCGGCGGTGAAATTATCGATGAGCGTGGTGGTTATGCCGATCG  
CGTCACACTACGTCTGAACGTCGAAAACCCGAAACTGTGGAGCGCCGAAATCCCCGAATCTCT  
ATCGTGCGGTGGTTGAACTGCACACCGCCGACGGCACGCTGATTGAAGCAGAAGCCTGCGA  
TGTCGGTTTCCGCGAGGTGCGGATTGAAAATGGTCTGCTGCTGCTGAACGGCAAGCCGTTGC  
TGATTCGAGGCGTTAACCGTCACGAGCATCATCCTCTGCATGGTCAGGTCATGGATGAGCAG  
ACGATGGTGCAGGATATCCTGCTGATGAAGCAGAACAACCTTTAACGCCGTGCGCTGTTGCGA  
TTATCCGAACCATCCGCTGTGGTACACGCTGTGCGACCGCTACGGCCTGTATGTGGTGGATG  
AAGCCAATATTGAAACCCACGGCATGGTGCCAATGAATCGTCTGACCGATGATCCGCGCTGG  
CTACCGGCGATGAGCGAACCGGTAACCGGAATGGTGCAGCGCGATCGTAATACCCGAGTG  
TGATCATCTGGTTCGCTGGGGAATGAATCAGGCCACGGCGCTAATCACGACGCGCTGTATCGC  
TGGATCAAATCTGTGATCCTTCCC GCCGGTG CAGTATGAAGGCGGCGGAGCCGACACCAC  
GGCCACCGATATTATTTGCCCGATGTACGCGCGCGTGGATGAAGACCAGCCCTTCCCGGCTG  
TGCCGAAATGGTCCATCAAAAAATGGCTTTCGCTACCTGGAGAGACGCGCCCGCTGATCCTT  
TGCGAATACGCCACGCGATGGGTAACAGTCTTGGCGGTTTCGCTAAATACTGGCAGGCGTT  
TCGTGAGTATCCCCGTTTACAGGGCGGCTTCGTCTGGGACTGGGTGGATCAGTCGCTGATTA  
AATATGATGAAAACGGCAACCCGTGGTTCGGCTTACGGCGGTGATTTTGGCGATACGCCGAA  
CGATCGCCAGTTCTGTATGAACGGTCTGGTCTTTGCCGACCGCACGCCGCATCCAGCGCTGA  
CGGAAGCAAAACACCAGCAGCAGTTTTTCCAGTTCCGTTTATCCGGGCAAACCATCGAAGTG  
ACCAGCGAATACCTGTTCCGTCATAGCGATAACGAGCTCCTGCACTGGATGGTGGCGCTGGA  
TGGTAAGCCGCTGGCAAGCGGTGAAGTGCCTCTGGATGTCGCTCCACAAGGTA AACAGTTG  
ATTGAACTGCCTGAACTACCGCAGCCGGAGAGCGCCGGGCAACTCTGGCTCACAGTACGCG  
TAGTGCAACCGAACGCGACCGCATGGTCAGAAGCCGGGCACATCAGCGCCTGGCAGCAGTG  
GCGTCTGGCGGAAAACCTCAGTGTGACGCTCCCCGCCGCTCCACGCCATCCCGCATCTGA  
CCACCAGCGAAATGGATTTTTGCATCGAGCTGGGTAAATAAGCGTTGGCAATTTAACCGCCAG  
TCAGGCTTTCTTTCACAGATGTGGATTGGCGATAAAAAACAACTGCTGACGCCGCTGCGCGA  
TCAGTTCACCCGTGCACCGCTGGATAACGACATTGGCGTAAGTGAAGCGACCCGCATTGACC

CTAACGCCTGGGTCTGAACGCTGGAAGGCGGGCCATTACCAGGCCGAAGCAGCGTTGTT  
GCAGTGCACGGCAGATACTTGTGATGCGGTGCTGATTACGACCGCTCACGCGTGGCAGC  
ATCAGGGGAAAACCTTATTTATCAGCCGAAAACCTACCGGATTGATGGTAGTGGTCAAATG  
GCGATTACCGTTGATGTTGAAGTGGCGAGCGATACCCGCATCCGGCGCGGATTGGCCTGAA  
CTGCCAGCTGGCGCAGGTAGCAGAGCGGGTAAACTGGCTCGGATTAGGGGCCGAAGAAAAC  
TATCCCGACCGCCTTACTGCCGCCTGTTTTGACCGCTGGGATCTGCCATTGTGACACATGTAT  
ACCCCGTACGTCTTCCCGAGCGAAAACGGTCTGCGCTGCGGGACGCGCGAATTGAATTATGG  
CCCACACCAGTGGCGCGGGCGACTTCCAGTTCAACATCAGCCGCTACAGTCAACAGCAACTGA  
TGGAAACCAGCCATCGCCATCTGCTGCACGCGGAAGAAGGCACATGGCTGAATATCGACGG  
TTTCCATATGGGGATTGGTGGCGACGACTCCTGGAGCCCGTCAGTATCGGCGGAATTCCAGC  
TGAGCGCCGGTCGCTACCATTACCAGTTGGTCTGGTGTCAAAAATAA

**Supplementary Table 5. Sequences of oligonucleotide probes used for *lacZ* mRNA molecules**

<b>Probes that bind to the head</b>	<b>Probes that bind to the tail</b>
GTGAATCCGTAATCATGGTC	TTTACCTTGTGGAGCGACAT
TCACGACGTTGTAAAACGAC	GTAGTTCAGGCAGTTCATC
TGCAAGGCGATTAAGTTGGG	TTGCACTACGCGTACTGTGA
TATTACGCCAGCTGGCGAAA	AGCGTCACACTGAGGTTTTTC
ATTCAGGCTGCGCAACTGTT	ATTTGCTGGTGGTCAGATG
AAACCAGGCAAAGCGCCATT	ACCCAGCTCGATGCAAAAAT
AGTATCGGCCTCAGGAAGAT	CGGTTAAATTGCCAACGCTT
AACCGTGCATCTGCCAGTTT	CTGTGAAAGAAAGCCTGACT
AATGGGATAGGTCACGTTGG	TTGTTTTTTATCGCCAATCC
GAACAAACGGCGGATTGACC	GTGCACGGGTGAACTGATCG
ATGTGAGCGAGTAACAACCC	ACTTACGCCAATGTCGTTAT
TAGCCAGCTTTCATCAACAT	CACTGCAACAACGCTGCTTC
AATAATTGCGTCTGGCCTT	CGCATCAGCAAGTGTATCTG
TTGCACCACAGATGAAACGC	AATAAGGTTTTCCCTGATG
TTCAGACGGCAAACGACTGT	CATCAATCCGGTAGGTTTTTC
CGCGTAAAAATGCGCTCAGG	CAACGGTAATCGCCATTTGA
TCCTGATCTTCCAGATAACT	AGTTTTCTTGCGGCCCTAAT
GAGACGTCACGGAAAATGCC	GTCAAAACAGGCGGCAGTAA
TGTGTAGTCGGTTTATGCAG	GGAAGACGTACGGGGTATAC
GGCAACATGGAAATCGCTGA	GTGGGCCATAATTCAATTCCG
CACATCTGAACTTCAGCCTC	TGATGTTGAACTGGAAGTCG
CACCTGCCATAAAGAAACT	TCAGTTGCTGTTGACTGTAG
CTCATCGATAATTCACCGC	AGATGGCGATGGCTGGTTTC
ACGTTCAGACGTAGTGTGAC	ATTCAGCCATGTGCCTTCTT
GCACGATAGAGATTCCGGGAT	AATCCCATATGGAAACCGT
	GAATTCCGCCGATACTGACG
	ACACCAGACCAACTGGTAAT

**Supplementary References**

- 1 Lutz, R. & Bujard, H. Independent and tight regulation of transcriptional units in *Escherichia coli* via the LacR/O, the TetR/O and AraC/I1-I2 regulatory elements. *Nucleic acids research* 25, 1203-1210 (1997).
- 2 Iyer, S., Park, B. R. & Kim, M. Absolute quantitative measurement of transcriptional kinetic parameters in vivo. *Nucleic acids research* 44, e142 (2016).
- 3 Svitil, A. L., Cashel, M. & Zyskind, J. W. Guanosine tetraphosphate inhibits protein synthesis in vivo. A possible protective mechanism for starvation stress in *Escherichia coli*. *Journal of Biological Chemistry* 268, 2307-2311 (1993).
- 4 Harinarayanan, R., Murphy, H. & Cashel, M. Synthetic growth phenotypes of *Escherichia coli* lacking ppGpp and transketolase A (tktA) are due to ppGpp-mediated transcriptional regulation of tktB. *Molecular microbiology* 69, 882-894 (2008).
- 5 Thomason, L. C., Costantino, N. & Court, D. L. *E. coli* genome manipulation by P1 transduction. *Current protocols in molecular biology / edited by Frederick M. Ausubel ... [et al.]* Chapter 1, Unit 1 17 (2007).
- 6 Datsenko, K. A. & Wanner, B. L. One-step inactivation of chromosomal genes in *Escherichia coli* K-12 using PCR products. *Proceedings of the National Academy of Sciences* 97, 6640-6645 (2000).
- 7 Reeve, C. A., Bockman, A. T. & Matin, A. Role of protein degradation in the survival of carbon-starved *Escherichia coli* and *Salmonella typhimurium*. *J. Bacteriol.* 157, 758-763 (1984).
- 8 Groat, R. G., Schultz, J. E., Zychlinsky, E., Bockman, A. & Matin, A. Starvation proteins in *Escherichia coli*: kinetics of synthesis and role in starvation survival. *J. Bacteriol.* 168, 486-493 (1986).
- 9 Reeve, C. A., Amy, P. S. & Matin, A. Role of protein synthesis in the survival of carbon-starved *Escherichia coli* K-12. *J Bacteriol* 160, 1041-1046 (1984).
- 10 Santos, J. M., Lobo, M., Matos, A. P. A., De Pedro, M. A. & Arraiano, C. M. The gene *bolA* regulates *dacA* (PBP5), *dacC* (PBP6) and *ampC* (AmpC), promoting normal morphology in *Escherichia coli*. *Molecular microbiology* 45, 1729-1740 (2002).
- 11 Johansen, J., Rasmussen, A. A., Overgaard, M. & Valentin-Hansen, P. Conserved Small Non-coding RNAs that belong to the  $\sigma^E$  Regulon: Role in Down-regulation of Outer Membrane Proteins. *Journal of molecular biology* 364, 1-8 (2006).
- 12 Souzu, H. Fluorescence polarization studies on *Escherichia coli* membrane stability and its relation to the resistance of the cell to freeze-thawing. I. Membrane stability in cells of differing growth phase. *Biochimica et Biophysica Acta (BBA) - Biomembranes* 861, 353-360 (1986).

- 13 Mengin-Lecreulx, D. & van Heijenoort, J. Effect of growth conditions on peptidoglycan content and cytoplasmic steps of its biosynthesis in *Escherichia coli*. *J. Bacteriol.* 163, 208-212 (1985).
- 14 Lam, H., Oh, D.-C., Cava, F., Takacs, C. N., Clardy, J., de Pedro, M. A. & Waldor, M. K. D-Amino Acids Govern Stationary Phase Cell Wall Remodeling in Bacteria. *Science* 325, 1552-1555 (2009).
- 15 Houser, J. R., Barnhart, C., Boutz, D. R., Carroll, S. M., Dasgupta, A., Michener, J. K., Needham, B. D., Papoulas, O., Sridhara, V., Sydykova, D. K., Marx, C. J., Trent, M. S., Barrick, J. E., Marcotte, E. M. & Wilke, C. O. Controlled Measurement and Comparative Analysis of Cellular Components in *E. coli* Reveals Broad Regulatory Changes in Response to Glucose Starvation. *PLoS computational biology* 11, e1004400 (2015).
- 16 Ballesteros, M., Fredriksson, A., Henriksson, J. & Nystrom, T. Bacterial senescence: protein oxidation in non-proliferating cells is dictated by the accuracy of the ribosomes. *The EMBO journal* 20, 5280-5289 (2001).
- 17 Dukan, S. & Nystrom, T. Bacterial senescence: stasis results in increased and differential oxidation of cytoplasmic proteins leading to developmental induction of the heat shock regulon. *Genes & development* 12, 3431-3441 (1998).
- 18 Kram, K. E. & Finkel, S. E. Culture Volume and Vessel Affect Long-Term Survival, Mutation Frequency, and Oxidative Stress of *Escherichia coli*. *Applied and environmental microbiology* 80, 1732-1738 (2014).
- 19 Gonidakis, S., Finkel, S. E. & Longo, V. D. Genome-wide screen identifies *Escherichia coli* TCA-cycle-related mutants with extended chronological lifespan dependent on acetate metabolism and the hypoxia-inducible transcription factor ArcA. *Aging cell* 9, 868-881 (2010).
- 20 Schellhorn, H. E. & Hassan, H. M. Transcriptional regulation of *katE* in *Escherichia coli* K-12. *J. Bacteriol.* 170, 4286-4292 (1988).
- 21 Chiancone, E. & Ceci, P. The multifaceted capacity of Dps proteins to combat bacterial stress conditions: Detoxification of iron and hydrogen peroxide and DNA binding. *Biochimica et Biophysica Acta (BBA) - General Subjects* 1800, 798-805 (2010).
- 22 Metzger, S., Schreiber, G., Aizenman, E., Cashel, M. & Glaser, G. Characterization of the *relA1* mutation and a comparison of *relA1* with new *relA* null alleles in *Escherichia coli*. *Journal of Biological Chemistry* 264, 21146-21152 (1989).
- 23 Gentry, D. R. & Cashel, M. Mutational analysis of the *Escherichia coli* *spoT* gene identifies distinct but overlapping regions involved in ppGpp synthesis and degradation. *Molecular microbiology* 19, 1373-1384 (1996).

- 24 Villadsen, I. S. & Michelsen, O. Regulation of PRPP and nucleoside tri and tetraphosphate pools in *Escherichia coli* under conditions of nitrogen starvation. *J. Bacteriol.* 130, 136-143 (1977).
- 25 Cashel, M. The Control of Ribonucleic Acid Synthesis in *Escherichia coli* : IV. RELEVANCE OF UNUSUAL PHOSPHORYLATED COMPOUNDS FROM AMINO ACID-STARVED STRINGENT STRAINS. *Journal of Biological Chemistry* 244, 3133-3141 (1969).
- 26 Murray, D. K. & Bremer, H. Control of spoT-dependent ppGpp Synthesis and Degradation in *Escherichia coli*. *Journal of molecular biology* 259, 41-57 (1996).
- 27 Lund, E. & Kjeldgaard, N. O. Metabolism of Guanosine Tetraphosphate in *Escherichia coli*. *European Journal of Biochemistry* 28, 316-326 (1972).
- 28 Chen, H., Shiroguchi, K., Ge, H. & Xie, X. S. Genome-wide study of mRNA degradation and transcript elongation in *Escherichia coli*. *Mol. Syst. Biol.* 11 (2015).
- 29 S Adhya, a. & Gottesman, M. Control of Transcription Termination. *Annual Review of Biochemistry* 47, 967-996 (1978).
- 30 Ray-Soni, A., Bellecourt, M. J. & Landick, R. Mechanisms of Bacterial Transcription Termination: All Good Things Must End. *Annual Review of Biochemistry* 85, 319-347 (2016).
- 31 Schmidt, M. C. & Chamberlin, M. J. Binding of rho factor to *Escherichia coli* RNA polymerase mediated by nusA protein. *Journal of Biological Chemistry* 259, 15000-15002 (1984).
- 32 Jin, D. J., Cashel, M., Friedman, D. I., Nakamura, Y., Walter, W. A. & Gross, C. A. Effects of Rifampicin resistant rpoB mutations on antitermination and interaction with nusA in *Escherichia coli*. *Journal of molecular biology* 204, 247-261 (1988).
- 33 Cardinale, C. J., Washburn, R. S., Tadigotla, V. R., Brown, L. M., Gottesman, M. E. & Nudler, E. Termination Factor Rho and Its Cofactors NusA and NusG Silence Foreign DNA in *E. coli*. *Science* 320, 935-938 (2008).
- 34 Mooney, R. A., Schweimer, K., Rösch, P., Gottesman, M. & Landick, R. Two Structurally Independent Domains of *E. coli* NusG Create Regulatory Plasticity via Distinct Interactions with RNA Polymerase and Regulators. *Journal of molecular biology* 391, 341-358 (2009).
- 35 Ha, K. S., Touloukhonov, I., Vassilyev, D. G. & Landick, R. The NusA N-Terminal Domain Is Necessary and Sufficient for Enhancement of Transcriptional Pausing via Interaction with the RNA Exit Channel of RNA Polymerase. *Journal of molecular biology* 401, 708-725 (2010).
- 36 Schmidt, M. C. & Chamberlin, M. J. nusA Protein of *Escherichia coli* is an efficient transcription termination factor for certain terminator sites. *Journal of molecular biology* 195, 809-818 (1987).
- 37 Burmann, B. M., Luo, X., Rösch, P., Wahl, M. C. & Gottesman, M. E. Fine tuning of the *E. coli* NusB:NusE complex affinity to BoxA RNA is required for processive antitermination. *Nucleic acids research* 38, 314-326 (2010).

- 38 Greive, S. J., Lins, A. F. & von Hippel, P. H. Assembly of an RNA-Protein Complex: BINDING OF NusB AND NusE (S10) PROTEINS TO boxA RNA NUCLEATES THE FORMATION OF THE ANTITERMINATION COMPLEX INVOLVED IN CONTROLLING rRNA TRANSCRIPTION IN ESCHERICHIA COLI. *Journal of Biological Chemistry* 280, 36397-36408 (2005).
- 39 Marr, M. T. & Roberts, J. W. Function of Transcription Cleavage Factors GreA and GreB at a Regulatory Pause Site. *Mol. Cell* 6, 1275-1285 (2000).
- 40 Feng, G. H., Lee, D. N., Wang, D., Chan, C. L. & Landick, R. GreA-induced transcript cleavage in transcription complexes containing Escherichia coli RNA polymerase is controlled by multiple factors, including nascent transcript location and structure. *Journal of Biological Chemistry* 269, 22282-22294 (1994).
- 41 Zhang, Y., Mooney, Rachel A., Grass, Jeffrey A., Sivaramakrishnan, P., Herman, C., Landick, R. & Wang, Jue D. DksA Guards Elongating RNA Polymerase against Ribosome-Stalling-Induced Arrest. *Mol. Cell* 53, 766-778 (2014).
- 42 Tehranchi, A. K., Blankschien, M. D., Zhang, Y., Halliday, J. A., Srivatsan, A., Peng, J., Herman, C. & Wang, J. D. The Transcription Factor DksA Prevents Conflicts between DNA Replication and Transcription Machinery. *Cell* 141, 595-605 (2010).
- 43 Sedlyarova, N., Rescheneder, P., Magán, A., Popitsch, N., Rziha, N., Bilusic, I., Epshtein, V., Zimmermann, B., Lybecker, M., Sedlyarov, V., Schroeder, R. & Nudler, E. Natural RNA Polymerase Aptamers Regulate Transcription in E. coli. *Mol. Cell* 67, 30-43.e36.
- 44 Zwiefka, A., Kohn, H. & Widger, W. R. Transcription termination factor rho: the site of bicyclomycin inhibition in Escherichia coli. *Biochemistry* 32, 3564-3570 (1993).
- 45 Csonka, L. N., Ikeda, T. P., Fletcher, S. A. & Kustu, S. The accumulation of glutamate is necessary for optimal growth of Salmonella typhimurium in media of high osmolality but not induction of the proU operon. *J Bacteriol* 176, 6324-6333 (1994).
- 46 Phaiboun, A., Zhang, Y., Park, B. & Kim, M. Survival Kinetics of Starving Bacteria Is Biphaseic and Density-Dependent. *PLoS computational biology* 11, e1004198 (2015).
- 47 Peterson, C. N., Mandel, M. J. & Silhavy, T. J. Escherichia coli starvation diets: essential nutrients weigh in distinctly. *J Bacteriol* 187, 7549-7553 (2005).
- 48 Wolfe, A. J. The acetate switch. *Microbiology and molecular biology reviews : MMBR* 69, 12-50 (2005).
- 49 Enjalbert, B., Cocaign-Bousquet, M., Portais, J.-C. & Letiche, F. Acetate Exposure Determines the Diauxic Behavior of Escherichia coli during the Glucose-Acetate Transition. *J. Bacteriol.* 197, 3173-3181 (2015).

- 50 Basan, M., Hui, S., Okano, H., Zhang, Z., Shen, Y., Williamson, J. R. & Hwa, T. Overflow metabolism in Escherichia coli results from efficient proteome allocation. *Nature* 528, 99-104 (2015).
- 51 Lange, R. & Hengge-Aronis, R. Identification of a central regulator of stationary-phase gene expression in Escherichia coli. *Molecular microbiology* 5, 49-59 (1991).
- 52 Kepes, A. Transcription and translation in the lactose operon of Escherichia Coli studied by in vivo kinetics. *Progress in Biophysics and Molecular Biology* 19, 199-236 (1969).
- 53 Schleif, R., Hess, W., Finkelstein, S. & Ellis, D. Induction Kinetics of the l-Arabinose Operon of Escherichia coli. *J. Bacteriol.* 115, 9-14 (1973).
- 54 Jin, D. J., Burgess, R. R., Richardson, J. P. & Gross, C. A. Termination efficiency at rho-dependent terminators depends on kinetic coupling between RNA polymerase and rho. *Proceedings of the National Academy of Sciences* 89, 1453-1457 (1992).
- 55 Proshkin, S., Rahmouni, A. R., Mironov, A. & Nudler, E. Cooperation Between Translating Ribosomes and RNA Polymerase in Transcription Elongation. *Science* 328, 504-508 (2010).
- 56 Dai, X., Zhu, M., Warren, M., Balakrishnan, R., Patsalo, V., Okano, H., Williamson, J. R., Fredrick, K., Wang, Y.-P. & Hwa, T. Reduction of translating ribosomes enables Escherichia coli to maintain elongation rates during slow growth. *Nature Microbiology* 2, 16231 (2016).
- 57 Chapman, A. G., Fall, L. & Atkinson, D. E. Adenylate Energy Charge in Escherichia coli During Growth and Starvation. *J. Bacteriol.* 108, 1072-1086 (1971).
- 58 Brauer, M. J., Yuan, J., Bennett, B. D., Lu, W., Kimball, E., Botstein, D. & Rabinowitz, J. D. Conservation of the metabolomic response to starvation across two divergent microbes. *Proceedings of the National Academy of Sciences* 103, 19302-19307 (2006).
- 59 Tosa, T. & Pizer, L. I. Biochemical Bases for the Antimetabolite Action of l-Serine Hydroxamate. *J. Bacteriol.* 106, 972-982 (1971).
- 60 Pizer, L. I. & Merlie, J. P. Effect of Serine Hydroxamate on Phospholipid Synthesis in Escherichia coli. *J. Bacteriol.* 114, 980-987 (1973).
- 61 Potrykus, K. & Cashel, M. (p)ppGpp: Still Magical? *Annual review of microbiology* 62, 35-51 (2008).
- 62 Haseltine, W. A. & Block, R. Synthesis of Guanosine Tetra- and Pentaphosphate Requires the Presence of a Codon-Specific, Uncharged Transfer Ribonucleic Acid in the Acceptor Site of Ribosomes. *Proceedings of the National Academy of Sciences* 70, 1564-1568 (1973).
- 63 Shyp, V., Tankov, S., Ermakov, A., Kudrin, P., English, B. P., Ehrenberg, M., Tenson, T., Elf, J. & Haurlyliuk, V. Positive allosteric feedback regulation of the stringent response enzyme RelA by its product. *EMBO reports* 13, 835-839 (2012).

- 64 Komissarova, N. & Kashlev, M. RNA Polymerase Switches between Inactivated and Activated States By Translocating Back and Forth along the DNA and the RNA. *Journal of Biological Chemistry* 272, 15329-15338 (1997).
- 65 Nudler, E., Mustaev, A., Goldfarb, A. & Lukhtanov, E. The RNA–DNA Hybrid Maintains the Register of Transcription by Preventing Backtracking of RNA Polymerase. *Cell* 89, 33-41 (1997).
- 66 Mamata, S. & Stefan, K. Backtracking dynamics of RNA polymerase: pausing and error correction. *Journal of Physics: Condensed Matter* 25, 374104 (2013).
- 67 Steitz, T. A. A structural understanding of the dynamic ribosome machine. *Nat Rev Mol Cell Biol* 9, 242-253 (2008).
- 68 Mechold, U., Potrykus, K., Murphy, H., Murakami, K. S. & Cashel, M. Differential regulation by ppGpp versus pppGpp in Escherichia coli. *Nucleic acids research* 41, 6175-6189 (2013).
- 69 Potrykus, K., Murphy, H., Philippe, N. & Cashel, M. ppGpp is the major source of growth rate control in E. coli. *Environmental microbiology* 13, 563-575 (2011).
- 70 Ryals, J., Little, R. & Bremer, H. Control of rRNA and tRNA syntheses in Escherichia coli by guanosine tetraphosphate. *J. Bacteriol.* 151, 1261-1268 (1982).
- 71 Cashel, M. & Gallant, J. Two Compounds implicated in the Function of the RC Gene of Escherichia coli. *Nature* 221, 838-841 (1969).
- 72 Epshtein, V., Kamarthapu, V., McGary, K., Svetlov, V., Ueberheide, B., Proshkin, S., Mironov, A. & Nudler, E. UvrD facilitates DNA repair by pulling RNA polymerase backwards. *Nature* 505, 372 (2014).
- 73 Kamarthapu, V., Epshtein, V., Benjamin, B., Proshkin, S., Mironov, A., Cashel, M. & Nudler, E. ppGpp couples transcription to DNA repair in E. coli. *Science* 352, 993-996 (2016).
- 74 Washburn, B. K. & Kushner, S. R. Construction and analysis of deletions in the structural gene (uvrD) for DNA helicase II of Escherichia coli. *J. Bacteriol.* 173, 2569-2575 (1991).
- 75 Ross, W., Vrentas, Catherine E., Sanchez-Vazquez, P., Gaal, T. & Gourse, Richard L. The Magic Spot: A ppGpp Binding Site on E. coli RNA Polymerase Responsible for Regulation of Transcription Initiation. *Mol. Cell* 50, 420-429 (2013).
- 76 Ross, W., Sanchez-Vazquez, P., Chen, Albert Y., Lee, J.-H., Burgos, Hector L. & Gourse, Richard L. ppGpp Binding to a Site at the RNAP-DksA Interface Accounts for Its Dramatic Effects on Transcription Initiation during the Stringent Response. *Mol. Cell* 62, 811-823 (2016).
- 77 Zuo, Y., Wang, Y. & Steitz, Thomas A. The Mechanism of E.coli RNA Polymerase Regulation by ppGpp Is Suggested by the Structure of their Complex. *Mol. Cell* 50, 430-436 (2013).

- 78 Cho, B.-K., Kim, D., Knight, E., Zengler, K. & Palsson, B. Genome-scale reconstruction of the sigma factor network in Escherichia coli: topology and functional states. *BMC Biol* 12, 1-11 (2014).
- 79 Dieterich, D. C., Link, A. J., Graumann, J., Tirrell, D. A. & Schuman, E. M. Selective identification of newly synthesized proteins in mammalian cells using bioorthogonal noncanonical amino acid tagging (BONCAT). *Proceedings of the National Academy of Sciences* 103, 9482-9487 (2006).
- 80 Beatty, K. E., Fisk, J. D., Smart, B. P., Lu, Y. Y., Szychowski, J., Hangauer, M. J., Baskin, J. M., Bertozzi, C. R. & Tirrell, D. A. Live-Cell Imaging of Cellular Proteins by a Strain-Promoted Azide–Alkyne Cycloaddition. *ChemBioChem* 11, 2092-2095 (2010).
- 81 Hatzenpichler, R., Scheller, S., Tavormina, P. L., Babin, B. M., Tirrell, D. A. & Orphan, V. J. In situ visualization of newly synthesized proteins in environmental microbes using amino acid tagging and click chemistry. *Environmental microbiology* 16, 2568-2590 (2014).
- 82 Soupene, E., van Heeswijk, W. C., Plumbridge, J., Stewart, V., Bertenthal, D., Lee, H., Prasad, G., Paliy, O., Charernnoppakul, P. & Kustu, S. Physiological studies of Escherichia coli strain MG1655: Growth defects and apparent cross-regulation of gene expression. *J. Bacteriol.* 185, 5611-5626 (2003).
- 83 Lyons, E., Freeling, M., Kustu, S. & Inwood, W. Using Genomic Sequencing for Classical Genetics in E. coli K12. *PloS one* 6, e16717 (2011).
- 84 Brown, S. D. & Jun, S. Complete Genome Sequence of Escherichia coli NCM3722. *Genome Announcements* 3 (2015).